

# P O L I M E R Y

CZASOPISMO POŚWIĘCONE CHEMII, TECHNOLOGII I PRZETWÓRSTWU POLIMERÓW

JAN RYBNICEK<sup>1), \*)</sup>, RALF LACH<sup>3), 4), 5)</sup>, WOLFGANG GRELLMANN<sup>5)</sup>, MONIKA LAPCIKOVA<sup>2)</sup>, MIROSLAV SLOUF<sup>2)</sup>, ZDENEK KRULIS<sup>2)</sup>, EVGENYI ANISIMOV<sup>1)</sup>, JIRI HAJEK<sup>1)</sup>

## Ternary PC/ABS/PMMA blends – morphology and mechanical properties under quasi-static loading conditions

**Summary** – PC/ABS/PMMA blends with a varied content of PMMA were studied. TEM microscopy was employed to reveal the individual phases. Uniaxial tensile testing and instrumented macro-hardness indentation were carried out to quantify the hardness, indentation modulus, elastic and plastic deformation work during indentation, yield strain and stress values. The data was correlated with the morphology. In case PMMA is the minor phase, it tends to locate on the PC/SAN interface; whereas in case of being the major one, SAN plays the role of compatibilizer and encapsulates the PC particles. Good compatibility of the blends was confirmed by the results of mechanical testing, which revealed strain-controlled plasticity.

**Keywords:** compatibilizer, morphology, ternary blend, polycarbonate, poly(methyl methacrylate), poly(acrylonitrile/butadiene/styrene), poly(styrene-co-acrylonitrile).

TRÓJSKŁADNIKOWA MIESZANINA PC/ABS/PMMA – MORFOLOGIA I WŁAŚCIWOŚCI MECHANICZNE W WARUNKACH OBCIĄŻENIA QUASI STATYCZNEGO

**Streszczenie** – Sporządzono mieszaniny poliwęglanu (PC) i kopolimeru akrylonitryl/butadien/styren (ABS) z różną zawartością poli(metakrylanu metylu) (PMMA). Metodą transmisyjnej mikroskopii elektronowej (TEM) zbadano morfologię próbek PC/ABS/PMMA, analizując strukturę fazową (rys. 1–3). W testach jednoosiowego rozciągania oceniano granicę plastyczności ( $\sigma_y$ ) oraz wydłużenie względne przy granicy plastyczności ( $\epsilon_y$ ) (rys. 4, 5). Na podstawie badań twardości metodą Martensa określano wartości pracy odkształcenia sprężystego ( $W_{el}$ ) i odkształcenia plastycznego ( $W_{pl}$ ) wytworzonych próbek z udziałem PMMA. Stwierdzono, że w przypadku dużej zawartości poli(metakrylanu metylu) w mieszaninie z PC/ABS, kopolimer poli(styren-co-akrylonitryl) (składnik ABS) pełni w układzie rolę kompatybilizatora, przyczyniając się do enkapsulacji cząstek PC, niewielka zaś ilość PMMA w mieszaninie powoduje międzyfazowe rozproszenie

<sup>1)</sup> Czech Technical University in Prague, Innovation Centre for Diagnostics and Application of Materials, Technická 4, 166 07 Prague 6, Czech Republic.

<sup>2)</sup> Institute of Macromolecular Chemistry, Academy of Science of the Czech Republic, Heyrovského nám. 2, 162 06 Praha 6, Czech Republic.

<sup>3)</sup> Institute of Polymer Materials, Geusaer Str. 88, Geb. 131, D-06217 Merseburg, Germany.

<sup>4)</sup> Vienna University of Technology, Institute of Materials Science and Technology, Favoritenstraße 9-11, A-1040 Vienna, Austria.

<sup>5)</sup> Martin-Luther University Halle-Wittenberg, Centre of Engineering, 06099 Halle/Saale, Germany.

\*) Author for correspondence: e-mail: jrybnicek@gmail.com

jego cząstek w układzie PC/ABS. Dobrą kompatybilność składników mieszaniny potwierdzają jej korzystne właściwości mechaniczne.

**Słowa kluczowe:** kompatybilizator, morfologia, trójskładnikowa mieszanina, poliwęglan, poli(metakrylan metylu), poli(akrylonitryl-butadien-styren), poli(styren-co-akrylonitryl).

Recycling by means of melt blending is a common practice to improve mechanical properties of polymer waste [1, 2]. A PC/ABS/PMMA blend, which has high potential for polymer recycling in the automotive industry [3, 4] and elsewhere, is a complex blend consisting of four amorphous polymers: (i) polycarbonate – PC, (ii) poly(styrene-co-acrylonitrile) – SAN, (iii) poly(methyl methacrylate) – PMMA and (iv) polybutadiene – PB. (ABS consists of crosslinked PB particles grafted by styrene and acrylonitrile into SAN matrix). The good compatibility of PC/ABS is well known, and the blend is widely used in the plastics industry. The potential of PMMA to support the interfacial strength of PC/ABS has been observed in several papers.

Most scientific papers on this subject deal with ABS-rich compositions where either PC or PMMA is the minor phase. The changes in morphology and the mechanical properties of ternary ABS/PMMA/PC, where PC is the minor phase, were studied by Kim *et al.* [5, 6]. Based on the calculation of spreading coefficients and TEM observations, the authors stated that PMMA has a tendency to encapsulate PC and that these two components do not form dispersed phases separately in the SAN matrix. Additionally, most of the rubber particles were retained in the SAN, but some large particles migrated to the PMMA phase or they were interposed at the SAN/PMMA interface. The addition of PMMA to PC/ABS blends leads to positive synergisms of tensile modulus, yield stress and impact strength where the summary weight fraction of PMMA and PC has been set at 40 % [6]. Liu and Bertilson [7] reported that the addition of 10 % of PMMA to a blend of ABS/PC (65/35) containing 5 phr methacrylate-butadiene-styrene copolymer (MBS) does not depress the mechanical properties, because PMMA is mutually miscible with SAN, depending on the acrylonitrile (AN) level, and is compatible with PC. Since the elongation at break and the J-integral increased to some extent, it was anticipated that interfacial adhesion between ABS and PC was enhanced by adding PMMA. Based on fracture surface morphology analysis and notched impact strength testing, Jin *et al.* [8, 9] reported compatibility enhancement of the ABS/PC blend by adding 5 pph of PMMA. The improved adhesion of the ABS/PC interface by PMMA changed the fracture mechanism and reduced the notch sensitivity of the blends.

Enhanced interfacial wettability of PC/ABS blends modified by PMMA leading to a positive effect on mechanical properties was also observed in [10]. PMMA has the most pronounced effect of all additives used in [11] as compatibilizers in PC/ABS blends, resulting in the greatest domain size reduction during processing. Debier

*et al.* [12] found that PMMA resides on the PC/SAN (75/25) interface (SAN containing 31 % of AN), and noted that the AN content in the SAN plays a crucial role. At lower contents of AN (23 %), SAN and PMMA were found to be fully miscible; no phase separation occurred.

The aim of this paper is to focus on the morphology of the PC/ABS/PMMA blend with a varied content of PMMA, ranging from PMMA minor to PMMA major compositions. The compatibility of the blends will be quantified by tensile testing and instrumented macro-hardness testing.

## EXPERIMENTAL

### Materials

The model blends were produced from Polycarbonate PC – Lexan LS2 (GE Plastics), acrylonitrile-butadiene-styrene ABS – Cycolac X37 (GE Plastics), poly(methyl methacrylate) PMMA – Lucryl G88 (BASF). These materials are commonly used for the production of car rear lights. The ternary blends were prepared with a constant PC/ABS ratio of 75/25 and the content of PMMA was varied in steps by 5, 10, 25, 50 and 75 weight per cent.

### Preparation methods

The blends were dry pre-mixed and injection moulded into Charpy specimens with length = 80 mm, width = 10 mm and thickness = 4 mm using a Battenfeld 500 injection moulding machine. The melt and mould temperatures were kept at 245 °C and 60 °C, respectively. The back pressure and injection pressure were set to 10 and 130 bars. The materials were dried for a minimum of 6 hours at a temperature of 105 °C in a hot-air dryer.

### Methods of testing

– The morphology of PC/ABS/PMMA blends was observed on ultrathin slices, which were prepared at laboratory temperature from injection-moulded specimens using an Ultratome III 8800 ultra-microtome (LKB produkt AB, Sweden) equipped with a glass knife. The slices were stained with OsO<sub>4</sub> or RuO<sub>4</sub>. These staining reagents were used separately or in combination to achieve the best discriminability of the used polymers. Transmission electron microscopy (TEM) measurements were performed on a Tecnai G2 Spirit microscope (FEI, Czech Republic). All microphotographs were taken at acceleration voltage 120 kV and were recorded with a digital camera.

Brightness, contrast and gamma corrections were performed with standard software.

– The fracture surfaces of the broken tensile test samples were analysed by scanning electron microscopy (SEM). All samples were coated with gold (JEOL JEE-4x sputter coater), and were observed with the help of a JSM 7600F (field emission cathode).

– Yield stress  $\sigma_y$  and deformation at yield  $\varepsilon_y$  were measured by means of uniaxial Instron measuring equipment according to ISO 527 at a crosshead speed of 50 mm/min.

– The macro-indentation behaviour was determined using the Zwick ZHU 2.5 macro-hardness recording test machine. Both the loading and unloading speed were 1 mm/min (quasi-static loading conditions) and the relaxation time between loading and unloading was set to 2 s. The maximum useful load  $F_{max}$  was 150 N. Martens hardness HM and indentation modulus  $E_{IT}$  were calculated according to ISO 14577. Other parameters were determined on the basis of the load-indentation depth diagrams that were measured, e.g. the elastic and plastic work of deformation ( $W_{el}$  and  $W_{pl}$ ).  $W_{el}$  is equal to the area under the loading curve and  $W_{pl}$  is equal to the area between the loading and unloading curve of the load-indentation depth diagrams.

## RESULTS AND DISCUSSIONS

### Morphology

The morphology of PC/ABS/PMMA blends with a content of 10, 25 and 50 % of PMMA was studied. For all blends, the ratio between PC and ABS was kept constant at a value of 75/25 (it is well known that this binary composition exhibits optimum toughness). Various ways of sample contrasting were used. OsO<sub>4</sub> bonded on double bonds of polybutadiene (PB) in ABS, which appeared dark on the TEM images. RuO<sub>4</sub> coloured all polymers competitively; the colouring was dependent on the exposition period. The best resolution of the individual phases was achieved when the samples were exposed to the combined effect of RuO<sub>4</sub> and OsO<sub>4</sub>.

Fig. 1(a), a blend with 10 % of PMMA, shows ABS particles dispersed in the PC matrix. PMMA is the minor phase in this PC-rich blend. At higher magnification [Fig. 1(b)], it is most probable that the PMMA resides on the PC/SAN interface – more precisely on PC/SAN interface, improving the adhesion of both phases. Because PMMA is more compatible with PC than with SAN, and less compatible with the grafted rubber in the ABS, the PMMA phase moves towards the interface of PC and SAN, where it will behave as a compatibilizer [13]. The PMMA location at the interface decreases the interfacial tension between the PC/ABS phases, thereby being able to reduce the ABS domain size [14]. It has also been found that the PMMA location suppresses phase coalescence upon annealing [13]. Owing to the difficulty encountered

in distinguishing the PMMA phase via TEM, our TEM investigations have clearly confirmed the PMMA location by imaging at the PC/SAN interface for the first time for PC-rich PC/ABS/PMMA blends (this has only rarely been investigated: only in this study and in [13]).

At PMMA concentrations above 25 %, it is more evident that SAN and PMMA prefer to coexist with each other, rather than to be dispersed separately in the PC matrix [Fig. 1(c)]. The viscosities of the studied PMMA and ABS were almost identical, and were considerably lower than the viscosity of PC, which leads to preferential mixing of these two phases [15]. Also, the interfacial tension is lowest between PMMA and SAN and highest between PC and SAN [16] (see Table 1), i.e. PMMA is more compatible with SAN than with PC (compare also [13]).

**Table 1.** Interfacial tension between PC, SAN and PMMA at 270 °C [14]

Components	Interfacial tension, 10 <sup>-3</sup> N/m
PC/SAN	0.45
PC/PMMA	0.17
PMMA/SAN	0

In the blend with 50 % of PMMA, ABS and PC are dispersed phases and PMMA becomes a continuous matrix. In this case, SAN is the minor phase and takes the role of a compatibilizer. PC particles encapsulated by SAN could be visualized with the help of the combined staining effect of RuO<sub>4</sub> and OsO<sub>4</sub> [see Fig. 1(d)]. The encapsulation of PC particles by SAN in PC/ABS/PMMA blends was observed for the first time in this study.

It might be objected that compatibility effects in ternary PC/ABS/PMMA blends, which have been analyzed in the literature mostly in very narrow ranges of PMMA fraction (1–5 wt. % [13], 23–27 wt. % [5], 5 pph [8], and very rarely a more general range (PMMA fraction up to 40 % [6]), can easily be deduced from the results of many studies made on compatibility effects in binary blends (PC/ABS, PC/SAN, PMMA/SAN). In general, however, uncritical application of this approach may result in serious misinterpretation of the data. This is due to the fact that both PC and SAN, and also PMMA and SAN are partially miscible, which makes the morphology formation in PC/ABS/PMMA blends much more difficult to understand than the formation observed in binary blends, due to additional interactions between the blend components. To suggest the morphology of multiphase blends such as PC/ABS/PMMA, the concept of the spreading coefficient was introduced by Hobbs *et al.* [17, 18]. Based on this concept, Kim *et al.* [5, 6] found for ABS-rich PC/ABS/PMMA blends that the PMMA phase has a tendency to envelop the PC, and that these two components do not form dispersed phases separately in the SAN matrix, well in agreement with their TEM investigations.

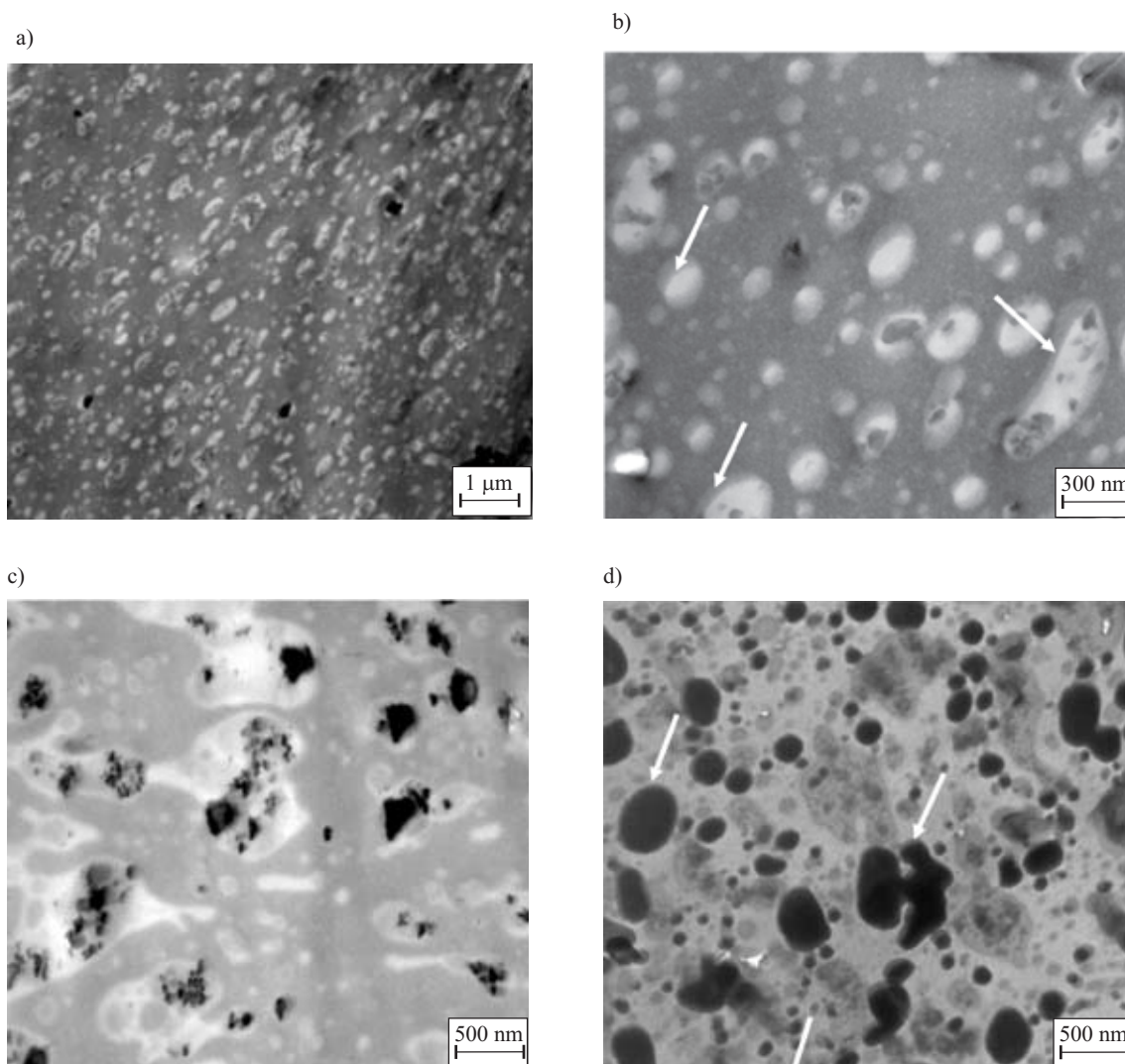


Fig. 1. Morphology of PC/ABS/PMMA blends: (a) Blend with 10 % PMMA: PC matrix (dark) with dispersed particles of ABS (grey); (b) Magnified view of (a): PC matrix (dark) with dispersed particles of ABS [SAN (light grey) and PB (dark)], PMMA (white arrows) most probably resides on the PC/SAN interface; (c) Blend with 25 % PMMA: PC matrix (grey), SAN (light grey) and PB (dark) coexist with PMMA (light); (d) Blend with 50 % PMMA: PMMA matrix (light grey), particles of PC (dark) and ABS [SAN (grey) and PB (dark)], SAN (white arrows) resides on the PC/PMMA interface. Staining procedure: (a) and (b) 10 min  $\text{RuO}_4$  + 90 min  $\text{OsO}_4$ , (c) 90 min  $\text{OsO}_4$ , (d) 60 min  $\text{RuO}_4$  + 90 min  $\text{OsO}_4$

Though the authors are well aware that molecular weight and polydispersity of the blend components as well as the rubber content of the ABS and acrylonitrile (AN) content in SAN also influence the formation of the morphology and compatibility effects, the blend composition (*i.e.* the percentage of PC, ABS and PMMA) is a major factor. Upon the first approximation, three different types of morphology are typical for ternary PC/ABS/PMMA blends:

(i) for ABS-rich blends (9–29 % PC, 54–67 % ABS, 5–27 % PMMA) [5, 6, 8]: PC inclusions are dispersed inside the SAN matrix. PMMA has been found [5, 6] or may be assumed [8] at the PC/SAN interfaces.

(ii) for PC-rich blends and lower PMMA fraction (60–71 % PC, 20–24 % ABS, 5–20 % PMMA) (this study, [13]): PC forms the matrix in which core-shell particles are well dispersed. The core is either an ABS inclu-

sion or several coexisting ABS and PC inclusions surrounded by the PMMA shell (and at 25 % PMMA also some small single PC particles with a PMMA shell). The PMMA shell has been directly imaged in this study [see Fig. 1(b)] or indirectly deduced by Yang *et al.* [13].

(iii) for PC-rich blends and higher PMMA fraction (50 % PC, 17 % ABS, 33 % PMMA) (only this study): Coexisting ABS and PC particles are well dispersed inside a PMMA matrix and the PC particles are covered with SAN shell [see Fig. 1(d)].

As already discussed for ABS-rich blends in [5, 6], the morphology formation can be understood by analyzing spreading coefficient  $\lambda_{ij}$  for component  $j$  on component  $i$  in matrix  $k$  with  $\lambda_{ij} = \gamma_{jk} - \gamma_{ik} - \gamma_{ji}$  [17, 18], where  $\gamma_{ij}$  is the interfacial tension between components  $i$  and  $j$ . The spreading coefficients of all possible material combinations are calculated in Table 2, using the data for interfacial tension

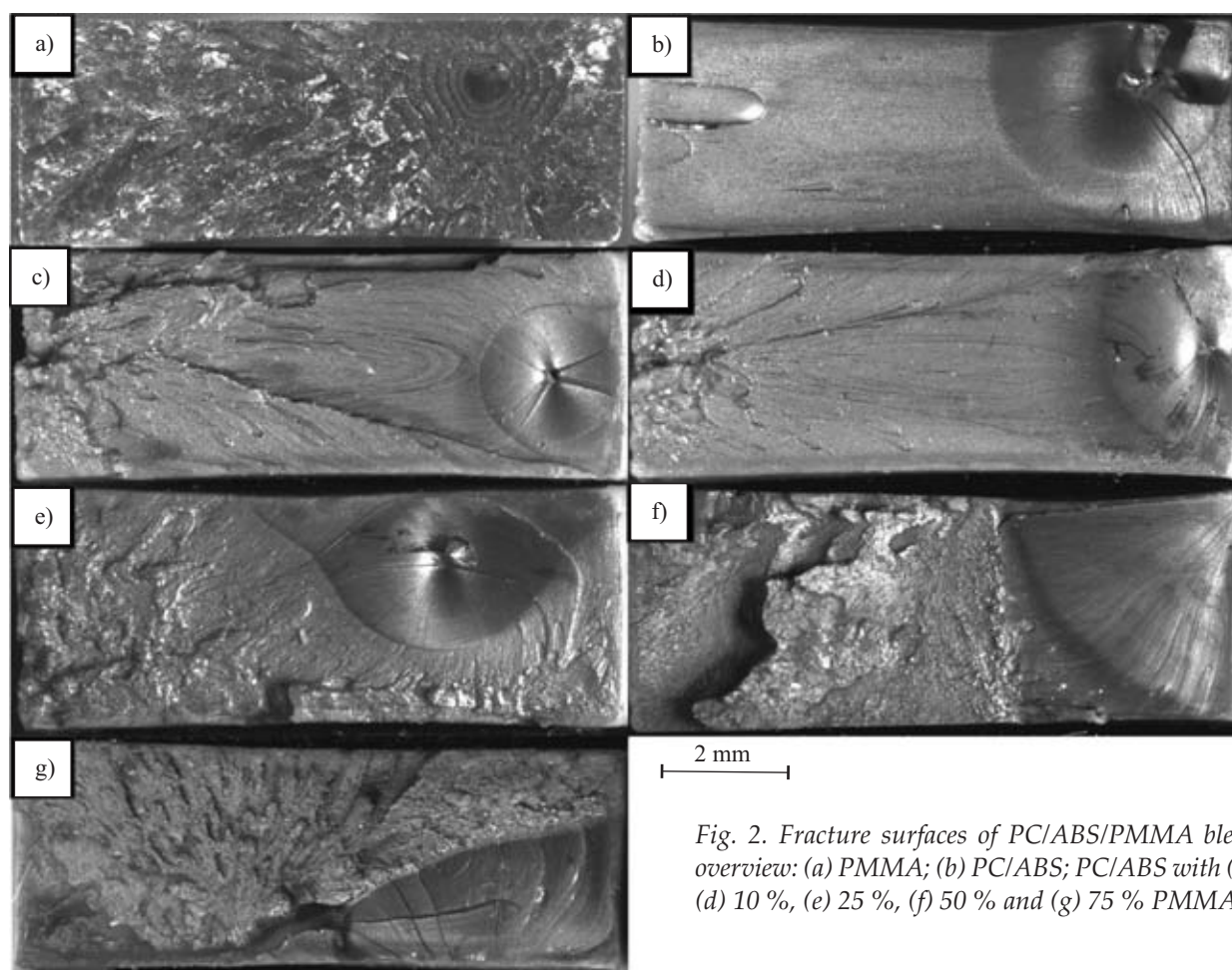


Fig. 2. Fracture surfaces of PC/ABS/PMMA blends — overview: (a) PMMA; (b) PC/ABS; PC/ABS with (c) 5 %, (d) 10 %, (e) 25 %, (f) 50 % and (g) 75 % PMMA

from [5, 6]. When  $\lambda_{ij}$  is positive, there is a tendency for component  $j$  to envelop component  $i$ , but if both  $\lambda_{ij}$  and  $\lambda_{ji}$  are negative the probability of the dispersed phase remaining separated is higher. Positive spreading coefficients  $\lambda_{PC/PMMA}$  (matrix: SAN, *i.e.* ABS) and  $\lambda_{PC/SAN}$  (matrix: PMMA) (see Table 2) confirm the observed blend morphologies (i) and (iii). In contrast, the spreading coefficients of material combinations with PC as matrix ( $\lambda_{PMMA/SAN}$ ,  $\lambda_{SAN/PMMA}$ ) are both negative, so according to the theory the PMMA and SAN should exist separately in PC matrix, which is inconsistent with the morphology (ii) observed by TEM [see Fig. 1(c)]. One reason for this may

be that the formation of the morphology is not only driven by the interfacial tension but also by the volume fraction of the blend components (as stated above as one of the major factors) and the viscosities of these components in the polymer melt.

### Mechanical properties under quasi-static loading conditions

Because our previous paper [15] mostly dealt with impact fracture behaviour and, in fact, the yield stress and yield strain of the PC/ABS/PMMA composed with 5 wt. % PMMA have only been coarsely sketched, a detailed analysis of the mechanical properties under quasi-static loading conditions should be provided in the present paper. From the authors' point of view, relatively little work has been done on the tensile properties of the PC/ABS/PMMA blends, often in a narrow range of blend composition (PMMA content: 1–5 wt. % [13], 23–27 % [5], up to 40 % [6]). However, data from tensile tests is needed for a comparison with the hardness data recorded during micro-hardness tests as one of the main parts of the paper.

Fig. 2 shows fracture surfaces of the tested blends with the following appearance: a) pure PMMA — only cleavage fracture in both initiation and propagation including crazing; b) PC/ABS blend — only shear yielding in both initia-

Table 2. Spreading coefficients calculated on the basis of interfacial tension ( $\gamma$ )<sup>a)</sup>

Matrix		Spreading coefficients
PMMA	SAN on PC	0.673
	PC on SAN	-6.703
SAN	PMMA on PC	0.673
	PC on PMMA	-0.769
PC	PMMA on SAN	-6.703
	SAN on PMMA	-0.769

<sup>a)</sup> Data of  $\gamma$  from [3, 4]:  $\gamma_{PC/SAN} = 3.015$ ,  $\gamma_{SAN/PMMA} = 3.736$ ,  $\gamma_{PC/PMMA} = 0.048$ .

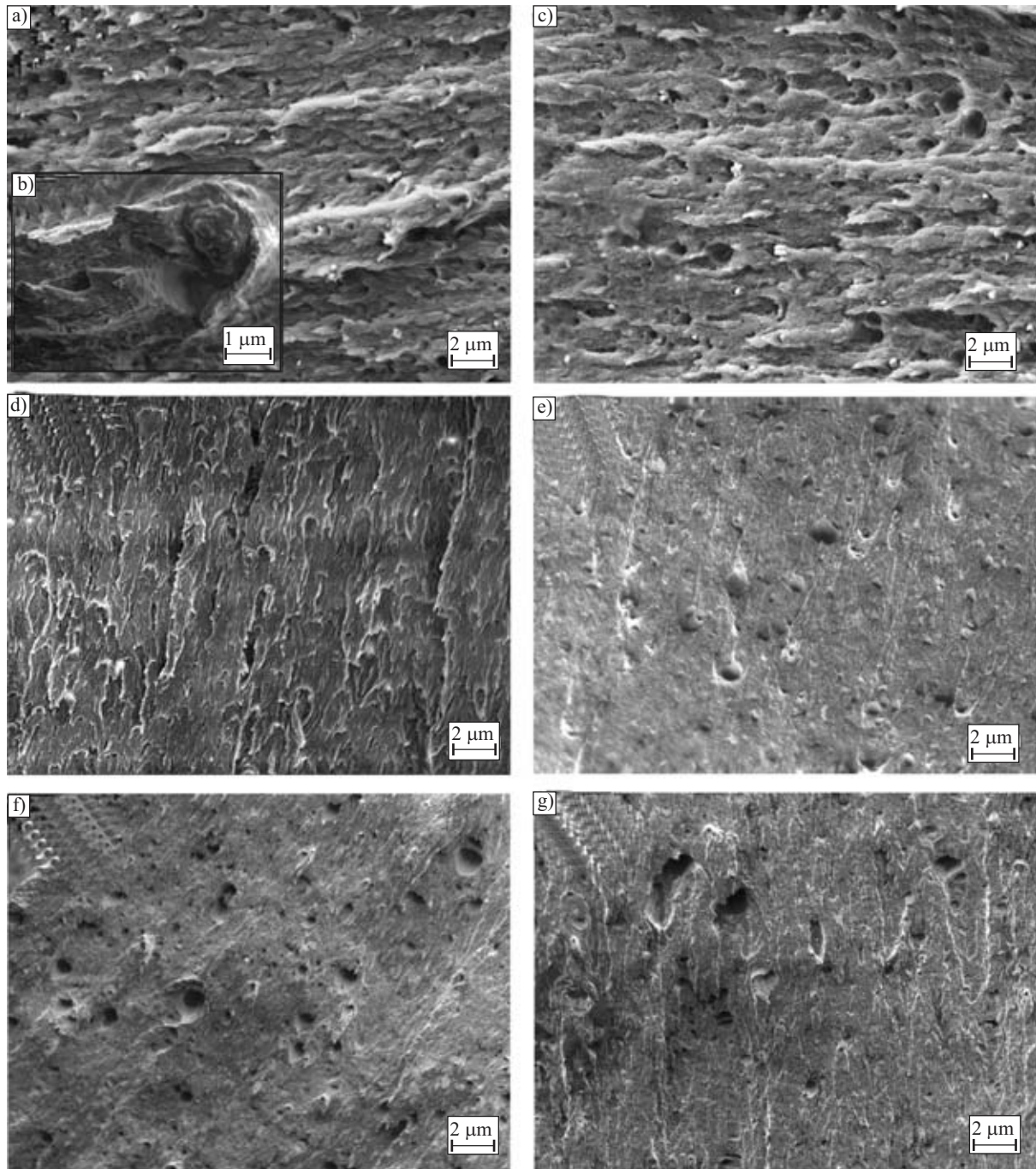


Fig. 3. Fracture surfaces of PC/ABS/PMMA blends — detailed view: (a) PC/ABS; (b) insert — enlarged view of plastic deformation around ABS particle; PC/ABS with (c) 5 %, (d) 10 %, (e) 25 %, (f) 50 % and (g) 75 % PMMA

tion and propagation; c) and d) PC/ABS blend with 5 % and 10 % of PMMA respectively — predominantly shear yielding (initiation and most parts of propagation); e), f) and g) PC/ABS blend with 25, 50 and 75 % of PMMA — shear yielding (only initiation) and cleavage fracture (propagation). Fig. 3 shows detailed view of the fracture initiation area. As the content of PMMA rises (ABS becomes minor phase) the amount of rubber cavitation decreases and the shear yielding is less pronounced (Fig. 3a–f).

The tensile test data for the PC/ABS/PMMA blend shows an increase in yield stress  $\sigma_y$  upon the addition of PMMA (Fig. 4). The data above the rule of mixtures sug-

gests good compatibility of all studied blends (the literature provides, the simplest relationship is the “rule of mixtures” which assumes a strong enough interfacial adhesion to ensure the stress transfer between the phases and that both phases are subject to the same deformation conditions, thus, the system responses will be determined by each phase volumetric proportion [19]). Yield strain  $\epsilon_y$  remains constant ( $\epsilon_y = 7.4\%$ ) independent of the PMMA content. This means that the onset of permanent plastic deformation is the strain controlled in a similar manner as previously observed for semicrystalline polymers [20]. Bubeck *et al.* [21] demonstrated for ABS that

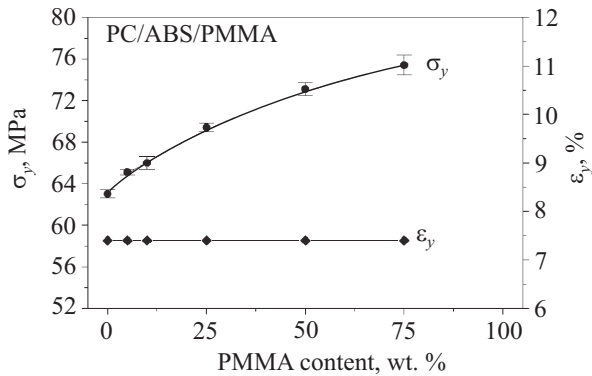


Fig. 4. Yield stress  $\sigma_y$  and yield strain  $\epsilon_y$  of PC/ABS/PMMA vs. PMMA content

the strain due to non-crazing mechanisms, such as rubber particle cavitation and deformation of the ligaments between rubber particles, occurs before the deformation due to crazing mechanisms. Also for PC/ABS [22], it has been found that crazing, albeit the precursor to final fracture, occurs after the predominant mechanism of rubber particle cavitation and shear deformation, and contributes only little to the total plastic deformation. The reasons why the plastic deformation of PC/ABS/PMMA blends is strain-controlled seems to be that rubber particle cavitation in the ABS phase is initiated at a well-defined critical strain (by exceeding the energy barrier for void formation [23]), followed by the deformation of SAN ligaments and shear deformation inside the PC phase. Any crazing in the PMMA phase therefore triggers only final fracture, *i.e.* the strain at break decreases upon addition of more than 10 % PMMA (Fig. 5), which clearly leads to reduced ductility of the blend. However, we have shown earlier that ternary blends, even when there are high contents of PMMA, maintain relatively good fracture toughness thanks to the toughening effects of PC/ABS [15, 24]. The ductile–brittle transition (DBT), when changing from dominant normal-stress induced deformation phenomena (such as crazing) to shear-stress induced phenomena (such as shear yielding), is strongly affected by test speed and external stress concentration

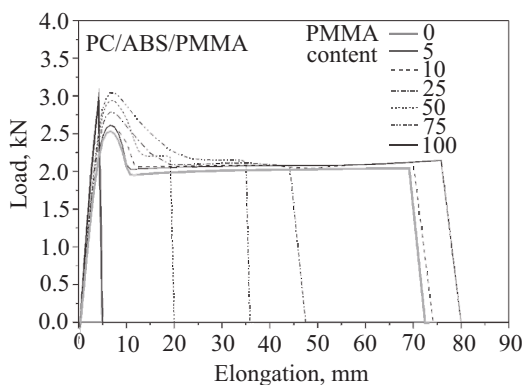


Fig. 5. Tensile test diagrams for PC/ABS/PMMA blends vs. PMMA content

(for example close to a crack). Hence, the DBT shifts from 10 % PMMA using the instrumented Charpy impact test (notched samples, test speed: 1 m/s) to >75 % PMMA at quasi-static loading using the uniaxial tensile test (test speed: 50 mm/min). As already said the strain at break is decreasing as a function of PMMA fraction whereas the stress at break remains constant (except neat PMMA) due to the same non-hardening stress–strain characteristics of all blends (also in [5] the ternary blends do not show any stress-hardening). However, the informational value of strain and stress at break must not put too much emphasis because both are not absolute material parameters but clearly affected by the qualities of the specimen surfaces and the compliance of the testing machine.

The Martens hardness (HM) and the indentation modulus ( $E_{IT}$ ) vs. PMMA content were found to be qualitatively comparable to the dependences of the yield stress measured with the help of the uniaxial tensile machine (compare Fig. 4 and Fig. 6). There are only a few references where hardness values are plotted versus the yield stress of polymers [25–28]. In most cases, the relationships are found to be linear with different slopes ranging from 2.33 [25] or 2.5 [26] or 2.8 [27] to 3 [22], depending on the method used for hardness measurement (Vickers

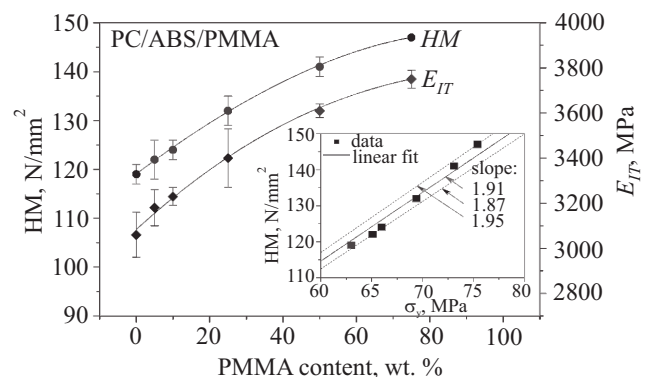


Fig. 6. Martens hardness and indentation modulus of PC/ABS/PMMA blends vs. PMMA content; correlation between yield stress and Martens hardness (insert)

hardness [25], hardness under load [26] or micro-hardness [22]). In our case, the slope is  $1.91 \pm 0.01$  (see insert in Fig. 6). The constant hardness-to-yield stress ratio approach has recently been criticised by Koch and Seidler [28]. Because the ratio of hardness values to tensile yield stress depends very strongly on the basic deformation mechanism (crazing, voiding or shear yielding) of the polymers, under tensile load they found no general linear relationship between hardness and yield stress. A closer inspection shows that the single  $HM/\sigma_y$  values of our materials increase slightly from 1.87 to 1.95 as a function of the PMMA weight fraction (see insert in Fig. 6). This observation can be correlated with the change of the predominant deformation mechanism from shear yielding

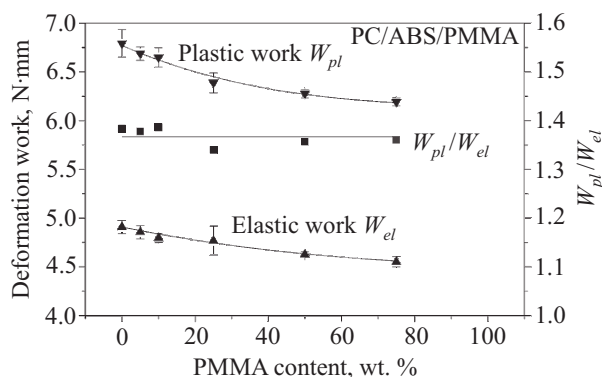


Fig. 7. Deformation behaviour of PC/ABS/PMMA blends vs. PMMA content

to crazing in PC/ABS/PMMA blends [15, 24], according to the results of Koch and Seidler for other polymers [28]. Thus, calculation of the yield stress from hardness must be done with more caution.

Instrumented macro-hardness measurement made it possible to determine the deformation work during indentation. Although both plastic work ( $W_{pl}$ ) and elastic work ( $W_{el}$ ) are clearly dependent on the composition of PC/ABS/PMMA blends, the general deformation behaviour characterized by the ratio  $W_{pl}/W_{el}$  is nearly constant and independent of the PMMA fraction (Fig. 7). Since work  $W$  is defined as  $W = \int F(h)dh$  ( $F$  — load,  $h$  — indentation depth), the constant  $W_{pl}/W_{el}$  ratio ( $W_{pl}/W_{el} = 1.37 \pm 0.02$ ) in the macro-indentation test has the same meaning as the material independent yield strain in the tensile test, *i.e.* the plastic deformation of PC/ABS/PMMA blends is strain-controlled, as discussed above.

## CONCLUSIONS

This work has characterized the morphology of a PC/ABS/PMMA blend with varied content of PMMA. PMMA and SAN were observed to preferentially coexist with each other rather than be dispersed separately in PC. In case of PMMA is the minor phase, it tends to locate on the PC/SAN interface, whereas in case of being the major phase, SAN plays the role of compatibilizer and encapsulates PC particles. The tensile test data, the yield stress and yield strain of PC/ABS/PMMA above the rule of mixtures suggest good compatibility of the blends. The Martens hardness ( $HM$ ), the indentation modulus ( $E_{IT}$ ) and the indentation elastic and plastic work versus PMMA content were found to be qualitatively comparable to the dependences measured by tensile testing. Both the constant yield strain (tensile test) and the constant ratio between elastic and plastic work (indentation test) independent of the PMMA weight fraction indicate that the plastic deformation of PC/ABS/PMMA blends is strain controlled.

## ACKNOWLEDGMENT

This work has been supported by the Ministry of Education, Youth and Sports of the Czech Republic, grant number

2B06097. The research has been carried out at the Innovation Centre for Diagnostics and Application of Materials at CTU in Prague (ICDAM), European Regional Development Fund, EU, CZ.2.16/3.1.00/21037.

## REFERENCES

1. Jeziórska R., Klepka T., Paukszta D.: *Polimery* 2007, **52**, 294.
2. Jeziórska R.: *Polimery* 2005, **50**, 468.
3. Pat WO 2 007 036 171 A1 20 070 405 (2007).
4. Horsch D., Blass R., Pfaff R.: *Kunststoffe* 1992, **82**, 1200.
5. Kim B. K., Yoon L. K., Xie X. M.: *J. Appl. Polym. Sci.* 1997, **66**, 1531.
6. Kim B. K., Choi C. G., Xie X. M.: *J. Macromol. Sci. Phys.* 1996, **B35**, 829.
7. Liu X., Bertelson H.: *J. Appl. Polym. Sci.* 1999, **74**, 510.
8. Jin D. W., Shon K. H., Jeong H. M., Kim B. K.: *J. Appl. Polym. Sci.* 1998, **69**, 533.
9. Jin D. W., Shon K. H., Jeong H. M.: *Polym. Korea* 1996, **20**, 775.
10. Choi K. J., Lee G. H., Ahn S. J., Shon K. H., Kim I., Jeong H. M.: *J. Appl. Polym. Sci.* 1996, **59**, 557
11. Yang K. M., Lee S. H., Oh J. M.: *Polym. Eng. Sci.* 1996, **23**, 1667.
12. Debier D., Devaux J., Legras R., Leblanc D.: *Polym. Eng. Sci.* 1994, **34**, 613.
13. Yang K., Lee Y. H., Oh J. M.: *Polym. Eng. Sci.* 1999, **39**, 1667.
14. Wu S.: *Polym. Eng. Sci.* 1978, **27**, 335.
15. Rybnicek J., Lach R., Lapcikova M., Seidl J., Krulis Z., Grellmann W., Slouf M.: *J. Appl. Polym. Sci.* 2008, **109**, 3210.
16. Cheng T. W., Keskkula H., Paul D. R.: *Polymer* 1992, **33**, 1606.
17. Hobbs S. Y., Dekkers M. E. J., Watkins V. H.: *Polymer* 1988, **29**, 1598.
18. Hobbs S. Y., Dekkers M. E. J., Watkins V. H.: *Polym. Bull.* 1987, **17**, 341.
19. Utracki L. A.: „Polymer Alloys and Blends: Thermodynamics and Rheology“, Hanser, Munich Vienna New York 1989.
20. Hobeika S., Men Y., Strobl G.: *Macromolecules* 2000, **33**, 1827.
21. Bubeck R. A., Buckley Jr. D. J., Kramer E. J., Brown H. R.: *J. Mater. Sci.* 1991, **26**, 6249.
22. Flores A., Balta-Calleja F. J., Attenburrow G. E., Bassett D. C.: *Polymer* 2000, **41**, 5431.
23. Bucknall C. B., Ayre D. S., Dijkstra D. J.: *Polymer* 2000, **41**, 5937.
24. Rybnicek J.: „Deformation and Fracture Behavior of Recycled PC, ABS, PMMA blends“, PhD Thesis, Czech Technical University, Prague 2007.
25. Weiler W.: „Härteprüfung an Metallen und Kunststoffen“, 2nd ed., Expert Verlag, Renningen 1990.
26. May M., Fröhlich F., Grau P., Grellmann W.: *Plaste Kautschuk* 1983, **30**, 149.
27. Herrmann K., Kompatschka M., Polzin T., Ullner C., Wehrstedt A.: „Härteprüfung an Metallen und Kunststoffen“, Expert-Verlag, Renningen 2007.
28. Koch T., Seidler S.: *Strain* 2009, **45**, 26.

Received 18 II 2011.